

A New Time Calibration Method for Switched-capacitor-array-based Waveform Samplers

H. Kim^{a,*}, C.-T. Chen^a, N. Eclov^a, A. Ronzhin^b, P. Murat^b, E. Ramberg^b,
S. Los^b, W. Moses^c, W.-S. Choong^c, C.-M. Kao^a

^a*Department of Radiology, University of Chicago, Chicago, IL 60637*

^b*Fermi National Accelerator Laboratory, Batavia, IL, US 60510*

^c*Lawrence Berkeley National Laboratory, Berkeley, CA, US 94720*

Abstract

We have developed a new time calibration method for the DRS4 waveform sampler that enables us to precisely measure the non-uniform sampling interval inherent in the switched-capacitor cells of the DRS4. The method uses the proportionality between the differential amplitude and sampling interval of adjacent switched-capacitor cells responding to a sawtooth-shape pulse. In the experiment, a sawtooth-shape pulse with a 40 ns period generated by a Tektronix AWG7102 is fed to a DRS4 evaluation board for calibrating the sampling intervals of all 1024 cells individually. The electronic time resolution of the DRS4 evaluation board with the new time calibration is measured to be \sim 2.4 ps RMS by using two simultaneous Gaussian pulses with 2.35 ns full-width at half-maximum and applying a Gaussian fit. The time resolution dependencies on the time difference with the new time calibration are measured and compared to results obtained by another method. The new method could be applicable for other switched-capacitor-array technology-

^{*}Corresponding author

Email address: `heejongkim@uchicago.edu` (H. Kim)

based waveform samplers for precise time calibration.

Keywords: Waveform Sampling, Time Calibration, Switched-Capacitors

1. Introduction

We are developing a high speed waveform sampling-based signal readout using the Domino-Ring-Sampler (DRS4) chip [1] for Time-of-Flight Positron Emission Tomography (TOF PET) [2][3]. In addition to precise time extraction, the use of a waveform sampling readout would result in simplified data acquisition hardware and a unified signal processing chain. Some of our signal readout approaches require a 10~20 ps RMS time resolution [3], and the electronic time resolution needs to be much better than that. It has been found that the DRS4 chip needs careful time calibration for individual capacitor cells in order to achieve precise time measurement within the entire time window it provides [4]. To illustrate this issue, Figure 1 shows the time resolution measurement using three different waveform readout electronics: the Tektronix 6154B digital scope (20 GS/s sampling, 15 GHz analog bandwidth), DRS4 evaluation board [5] (PSI, Switzerland), and PDRS4 [4](NOTICE, Korea and University of Chicago). The DRS4 evaluation board uses the time calibration method provided by PSI, and the PDRS4 uses a different time calibration method that we have previously reported [4]. The DRS4 result clearly shows a significant degradation in time resolution when the time difference increases. While our calibration method reduces such degradation, there is still room for improvement, especially for applications that require precise timing measurement. In contrast, such degradation is not observed with the Tektronix digital scope, which uses flash ADC tech-

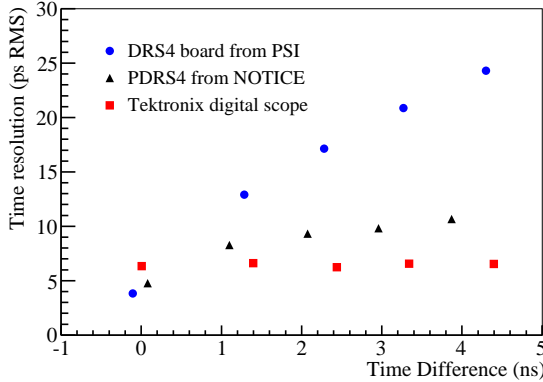


Figure 1: Electronic time resolution as a function of the time difference obtained by using two DRS4-based readout boards and a Tektronix digital oscilloscope. The dependence on the time difference observed in the DRS4-based boards is mainly due to inaccurate time calibration.

23 nology. Comparing the PDRS4 and Tektronix results also suggests that time
 24 resolution as precise as achieved by using the high-end commercial digital
 25 scopes could be achieved by using the DRS4 chips if their calibration can be
 26 performed properly.

27 In the DRS4 waveform sampling chip, the sampling interval between two
 28 successive capacitor cells is determined by the time delay of the inverters
 29 between them. The transistor variations in the chip cause the non-uniform
 30 sampling intervals unlike using flash ADC-based waveform sampling. If not
 31 properly calibrated, the non-uniform sampling interval results in a time res-
 32 olution dependence on the time difference as shown in Figure 1: as the time
 33 difference increases, more samples are involved and the errors in their time
 34 intervals accumulates to degrade the resolution of the time measurement.
 35 The current time calibration method implemented in the DRS4 evaluation

36 board Version 4 by its developer [6] uses a 132 MHz clock signal for time cali-
37 bration (hereafter we refer to it as the DRS4 Eval V4 method).¹ This method
38 initially assumes an uniform time interval for all capacitor cells, e.g., 200 ps
39 at 5 GS/s. From the recorded waveform of the 132 MHz clock, zero-crossing
40 points on rising/falling waveforms are calculated, and the time intervals be-
41 tween two adjacent zero-crossing points are compared to the known clock
42 period. The deviations of the calculated time intervals from the clock period
43 are applied as a correction to the capacitor cells within two zero-crossing
44 points. The sampling interval for each capacitor cell is obtained iteratively
45 by repeating the procedure.

46 However, the non-uniform sampling intervals of the DRS4 are not re-
47 vealed clearly by the DRS4 Eval V4 method because the time calculation
48 and correction in the method involves multiple capacitor cells (e.g., \sim 38 cells
49 at 5 GS/s), and the difference between cells could be averaged out as a result.
50 We have developed a new time calibration method to individually measure
51 the sampling interval associated with each capacitor cell of the DRS4. Our
52 method uses a sawtooth-shape pulse as a calibration source, which is linearly
53 increasing/decreasing in amplitude and time coordinate (hereafter we refer
54 to it as the Sawtooth method). Since the slope of the input pulse is kept the
55 same regardless of the sampling instance, the measured amplitude difference
56 between two adjacent sampled points is proportional to the sampling interval
57 between two cells. By using this proportionality, the sampling interval can be

¹After submitting the manuscript, the next version (V5) of the DRS4 evaluation board was announced, and improved performances relative to the V4 including time resolution are claimed in the DRS4 web page.

58 determined individually from the differential amplitude for all the capacitor
59 cells. Currently, several high-speed waveform sampling ASICs [7][8][9] based
60 on the switched-capacitor cell technology are available in addition to the
61 DRS4, and several time calibration methods developed for those ASICs have
62 been reported in the literature [9][10][11][12]. Among them, the method [10]
63 by Breton *et al.* is similar to our approach: the sampling interval is extracted
64 from a segment of a sine wave around a zero-crossing point while assuming
65 linearity of the sine wave in the segment. In our method, such an assump-
66 tion on the linearity of the calibration source is not necessary, and all of the
67 rising/falling portion of the sawtooth-shape pulse is exploited in calibration.

68 In this study, the DRS4 evaluation board V4 is used for the experimen-
69 tal tests to compare the results obtained by applying the two different time
70 calibration methods: the DRS4 Eval V4 method and the Sawtooth method.
71 The calibration method, experimental test set-up, and time resolution mea-
72 surements are presented in the following sections.

73 2. Method

74 Figure 2(a) illustrates how a linearly increasing pulse is used for our time
75 calibration method. For simplicity, only three sampled points in amplitude
76 and time coordinate are marked by red circles on the straight line, which is
77 a segment of the input pulse to the DRS4. In the figure, ΔV , the differential
78 amplitude between two adjacent samples, is proportional to Δt , the sampling
79 interval between them. The ratio between ΔV and Δt is the slope of the
80 pulse and is the same for ΔV measurements obtained by all 1024 capacitor
81 cells as shown in Equation 1, where the subscript i is added to ΔV and

82 Δt to refer to the measurements obtained by the i th capacitor cell. In the
 83 DRS4, the entire sampling interval of the 1024 capacitor cells is fixed by
 84 an on-chip phase-locked loop (PLL) circuit, e.g., 200 ns at 5 GS/s. This
 85 constraint, as shown in Equation 2, makes it possible to calculate the single
 86 normalization factor, C , from the sum of ΔV_i . Equation 3 expresses the
 87 sampling interval determined by using the conversion factor and measured
 differential amplitude for each capacitor cell.

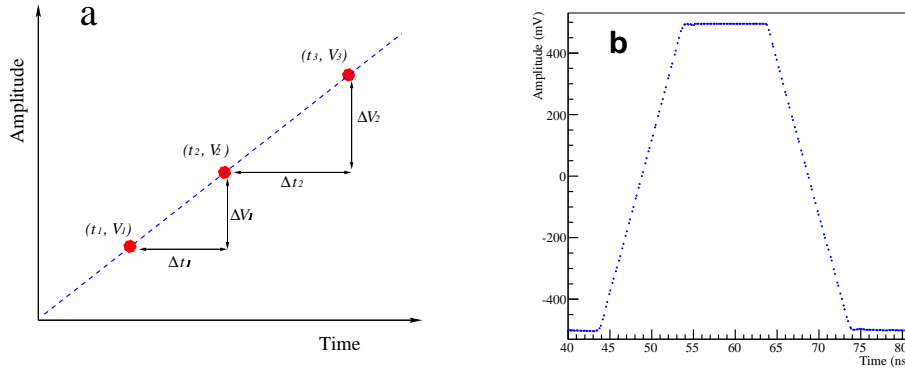


Figure 2: (a) Sampled waveform on a linearly increasing pulse. The (non-uniform) sampling interval Δt_i is proportional to the differential amplitude ΔV_i . (b) A Sawtooth-shape waveform with 40 ns period generated by the Tektronix AWG7102.

88

$$C = \frac{\Delta V_1}{\Delta t_1} = \frac{\Delta V_2}{\Delta t_2} = \dots = \frac{\Delta V_i}{\Delta t_i} \quad (1)$$

89

$$\sum_{i=0}^{1023} \Delta V_i = C \sum_{i=0}^{1023} \Delta t_i = C \times 200 \text{ ns} \quad (2)$$

90

$$\Delta t_i = \frac{\Delta V_i}{C} = \frac{\Delta V_i}{\sum_{i=0}^{1023} \Delta V_i} \times 200 \text{ ns} \quad (3)$$

91 Figure 2(b) shows the sawtooth-shape pulse used in the calibration. Each
 92 portion of the pulse (rising/falling and plateau) has 10 ns duration, yielding
 93 a 40 ns period in one cycle. The slope at the rising/falling part of the pulse
 94 is fixed to be $+100/-100$ mV/ns, and the amplitude of the pulse covers the
 95 full dynamic input range of the DRS4.

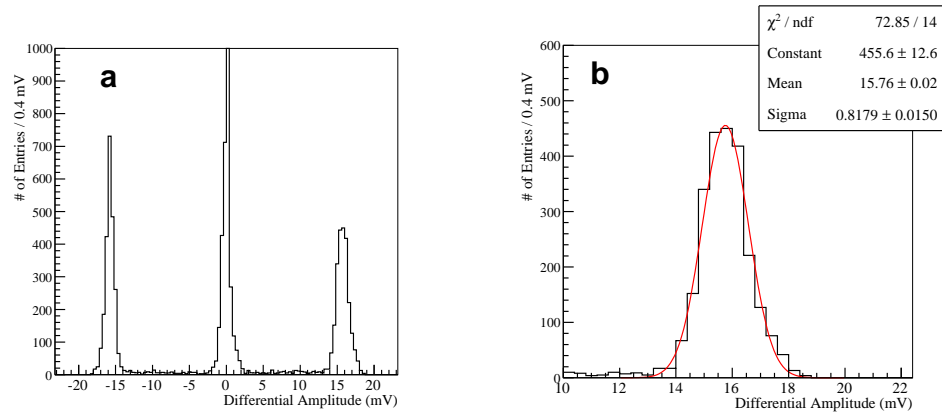


Figure 3: (a) A histogram of the differential amplitude (ΔV) obtained at a particular capacitor cell obtained by sending 10K sawtooth-shape pulses to the DRS4 evaluation board. (b) Fitting of the positive peak in (a) to a Gaussian function.

96 Figure 3 shows a histogram of the measured differential amplitudes at a
 97 particular capacitor cell obtained by sending 10,000 (10K) sawtooth-shape
 98 pulses to the DRS4 evaluation board. The peaks centered at approximately
 99 $+16/-16$ mV represent when the particular capacitor cell is in the rising/falling
 100 portion of the pulse. Similarly, the plateau of the pulse produces the peak at
 101 0 mV. We include the plateau to produce such a center peak in the histogram
 102 for verifying whether the measurement procedure works properly. Since this
 103 center peak is not used in calibration, the plateau of the pulse can be reduced
 104 or removed completely. In addition to the peaks, small tails between peaks

105 are observed. These tails represent when the cell is in the transition regions
 106 between the rising/falling portion and the plateau of the pulse. Using this
 107 histogram, ΔV measured by a particular capacitor cell for the rising/falling
 108 portion of the sawtooth-shape pulse is obtained by averaging the center lo-
 109 cations of the positive and negative peaks as determined, as illustrated by
 110 Figure 3(b), by Gaussian fitting. From this average ΔV , the sampling time
 111 interval Δt associated with the capacitor cell, referred to as the *time cal-
 112 ibration constant* below, is obtained by applying the measured conversion
 113 constant C as described above.

114 3. Experimental Setup

115 The block diagram of the time calibration set-up is depicted in Fig-
 116 ure 4(a). The sawtooth-shape pulse with 40 ns period is generated by using
 117 a Tektronix AWG7102 waveform generator [13] and fed to one input channel
 118 of the DRS4 evaluation board. The AWG7102 is an arbitrary waveform gen-
 erator with 10 GS/s sampling and ~ 1 ps random jitter. For the waveform

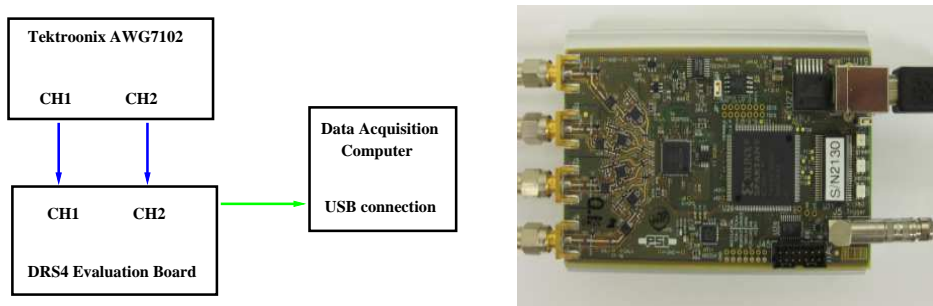


Figure 4: (a) A block diagram of experimental setup. Pulses generated by the AWG7102
 are sampled by a DRS4 evaluation board, and the waveforms digitized by the DRS4 are
 transferred to a computer through USB interface. (b) DRS4 evaluation board (PSI).

119

120 digitizer, a DRS4 evaluation board (PSI) is used. The DRS4 board, shown in
121 Figure 4(b), provides 4 input channels, each with 1024 capacitor cells. The
122 input dynamic range of the DRS4 chip is 1 V (-0.5 to 0.5 V), and the sam-
123 pling speed is adjustable from 0.7 to 5 GS/s. Since the DRS4 provides a full
124 sampling range of 200 ns, a 6 cycle-long sawtooth-shape pulse is used in each
125 calibration event, and as mentioned above 10K events are used for the ΔV
126 measurement. Digitized waveforms acquired by the DRS4 board are trans-
127 ferred to a computer for off-line analysis. The evaluation board is equipped
128 with on-board amplitude and time calibration software, and it makes it pos-
129 sible to perform a comparison study between two time calibration methods
130 using the same waveform data set: only the time information is switched
131 while the amplitude of the waveform is kept the same. For measuring the
132 electronic time resolution, two identical Gaussian pulses ($\sigma = 1$ ns, 500 mV
133 amplitude) are generated by the AWG7102 and are connected to two input
134 channels of the DRS4 board. The time difference between these two Gaussian
135 pulses is varied by programming the AWG7102.

136 **4. Results**

137 *4.1. Time calibration using sawtooth-shape pulse*

138 Figure 5 compares the differential amplitude histograms obtained for ca-
139 pacitor cell #0 and #1 by using 10K sawtooth-shape pulses. Following the
140 procedure described in Section 2, the ΔV values are determined to be 15.0
141 mV and 23.8 mV for cell id#0 and #1, respectively. Such a significant dif-
142 ference in ΔV is observed between the odd- and even-numbers cells of the

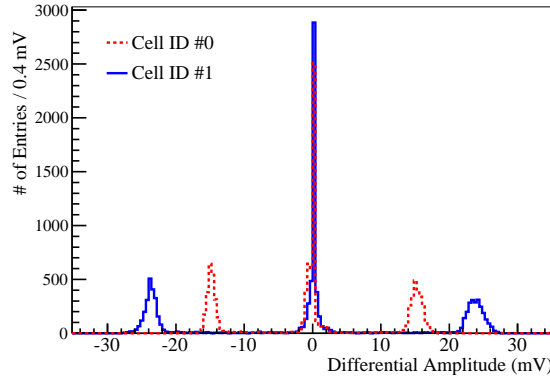


Figure 5: Differential amplitude ΔV histogram obtained for the capacitor cell id#0 and 1. Such significant differences in the ΔV measurement are observed between the odd- and even-numbered capacitor cells of the DRS4.

¹⁴³ DRS4.

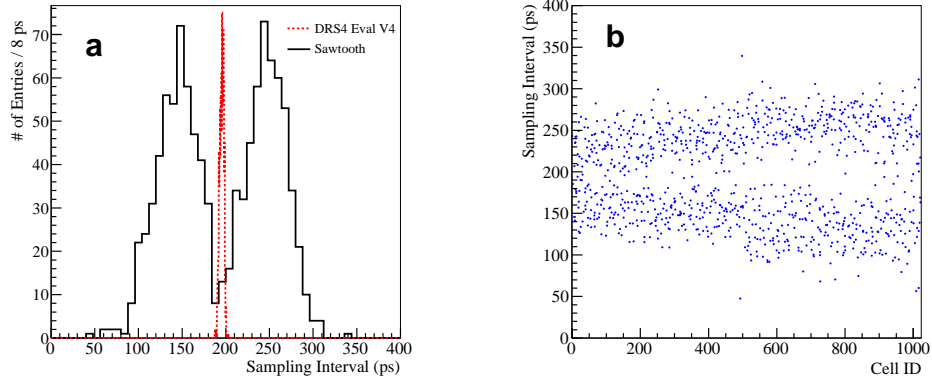


Figure 6: (a) Histograms of the sampling interval (time calibration constant) obtained for the 1024 capacitor cells of the DRS4 by using the DRS4 Eval V4 method and the Sawtooth method. (b) A scatter plot of the sampling intervals obtained by the Sawtooth method.

¹⁴⁴ Figure 6(a) shows the histograms of the sampling intervals (the time cali-

145 bration constants) obtained for the 1024 cells of the DRS4 by using the Saw-
 146 tooth method and the DRS4 Eval V4 method. With the Sawtooth method,
 147 the time calibration constant has two distinct groups, reflecting the difference
 148 between the odd- and even-numbered cells. The means (widths) of these two
 149 groups are 142.2 ps and 245.8 ps (24.8 ps RMS and 24.8 ps RMS), respec-
 150 tively. The scatter plot in Figure 6(b) reveals a more systematic pattern of
 151 the time calibration constants: in addition to the difference in odd- and even-
 152 numbered cells, the difference between the first half (#0-511) and second half
 153 (#512-1023) can also be observed. These patterns are consistent with the
 154 observation recently reported by Shaver et al in which another calibration
 155 method is used [14]. Unlike the Sawtooth method, Figure 6(a) also shows
 156 that the time calibration constants generated by the DRS4 Eval V4 method
 157 are very similar for 1024 capacitor cells: the mean of the distribution is 195.3
 158 ps and the RMS is only 2.4 ps.

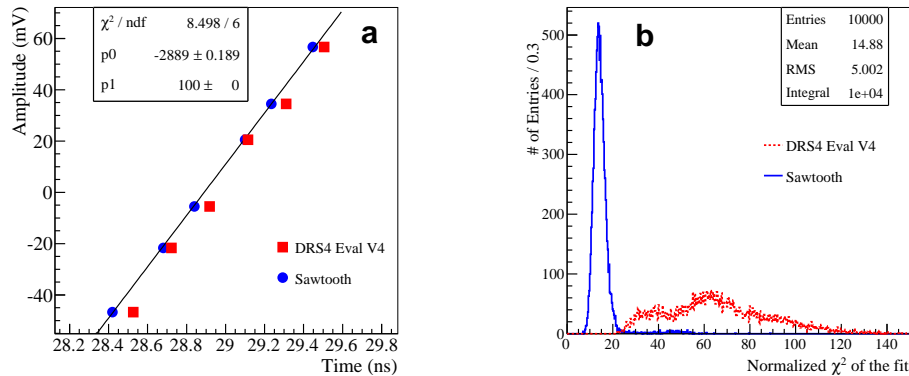


Figure 7: (a) A segment of sawtooth-shape waveform using two sets of time calibrations. A straight line fit on the waveform is shown (~0.5 mV error bar is too small to be seen in the figure.) (b) Normalized χ^2 of the fit using two sets of time calibrations.

159 The resulting time calibration constants are applied to a separately ac-
160 quired dataset for the sawtooth-shape pulse to evaluate how well the linearity
161 of the rising portion of the pulse is reproduced. Figure 7(a) shows a close-up
162 of the a segment of the rising portion of the sawtooth-shape pulse measured
163 by the DRS4 evaluation board by using the time calibration constants deter-
164 mined by the DRS4 Eval V4 method and Sawtooth method. The samples
165 are fitted with a straight line with a slope of 100 mV/ns, which is the known
166 slope of the segment. It should be noted that the samples of the two meth-
167 ods have the same amplitudes. From the fitting shown in Figure 7(a), it is
168 clearly seen that the samples obtained by the Sawtooth method recover the
169 input pulse better than the samples obtained by the DRS4 Eval V4 method.
170 The straight-line fit is carried out for 10K waveform samples in a -450 mV
171 to 450 mV range, and the normalized χ^2 distributions of the fit (degree of
172 freedom in the fit is approximately equal to 47) obtained for the time cali-
173 bration methods are compared in Figure 7(b). In comparison with the DRS4
174 Eval V4 method, the χ^2 error of the Sawtooth method is much smaller in
175 magnitude and much narrower in distribution.

176 4.2. Electronic time resolution measurement using Gaussian pulses

177 To evaluate the electronic timing resolution, two identical Gaussian pulses
178 are generated from two channels of the Tektronix AWG7102 waveform gen-
179 erator and sent to two input channels of the DRS4 evaluation board. The
180 time difference between the occurrence of the two Gaussian pulses are varied
181 from 0 ns to 170 ns to investigate the dependence of the time resolution on
182 the time difference. Figure 8(a) shows the samples acquired for the Gaus-
183 sian pulses with a 5.0 ns time difference. A Gaussian fit is applied to the

184 waveforms recorded, and the center location of the Gaussian fit is taken as
 185 the event time. Figure 8(b) shows the time difference measurement using
 186 the two Gaussian pulses with 1.0 ns time difference between them. Both the
 187 DRS4 Eval V4 method and the Sawtooth method yield a mean value of 0.89
 188 ns; the deviation from the known value of 1.0 ns can be attributed to the
 189 slight cable difference. Since the distribution is not Gaussian, the width of
 190 the distribution is evaluated by using RMS. The time resolution is measured
 191 to be about 2.9 ps RMS with the Sawtooth method and about 8.1 ps RMS
 192 with the DRS4 Eval V4 method.

193 The time resolution dependence on the time difference between the Gaus-
 194 sian pulses is shown in Figure 9(a). Compared to the results using the DRS4

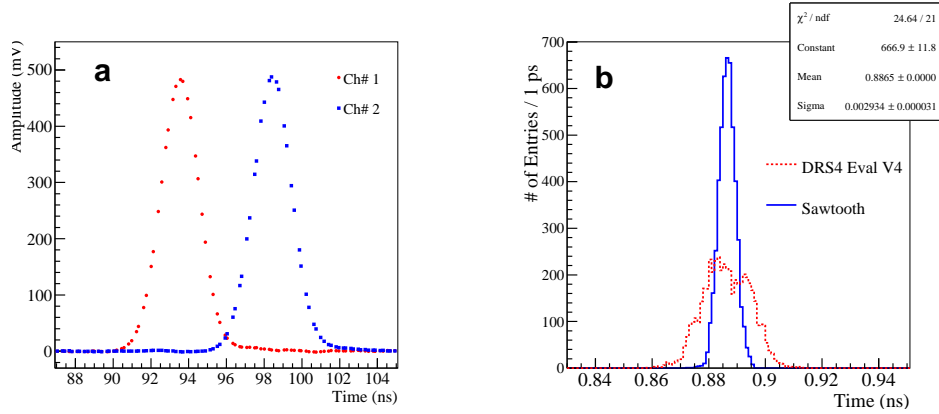


Figure 8: (a) Sampled waveforms obtained by the DRS4 board for two identical Gaussian pulses with a time difference of 5.0 ns (generated by an AWG7102 waveform generator). (b) Histograms of the measured time difference when the time difference between the Gaussian pulses is 1.0 ns. The time resolution is estimated to be about 2.9 ps RMS and 8.1 ps RMS when using the time calibration constants obtained by the Sawtooth method and the DRS4 Eval V4 method, respectively.

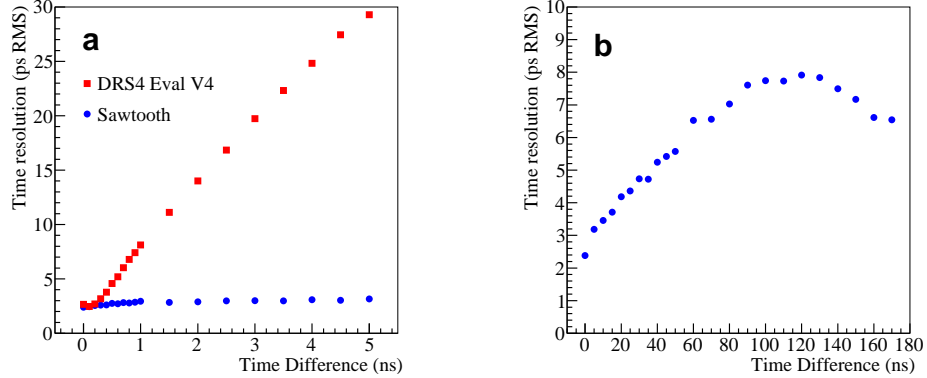


Figure 9: (a) The electronic time resolution as the time difference varies from 0 to 5 ns. (b) The time resolution with time difference up to 170 ns shows its dependence on the time difference.

195 Eval V4 method, the time resolution dependence on the time difference is
 196 negligible with the Sawtooth method (29.3 ps RMS vs. 3.2 ps RMS at 5.0 ns
 197 time difference). The time resolution dependence of the Sawtooth method
 198 measured with time difference up to 170 ns is shown in Figure 9(b). The
 199 resolution degrades as the time difference increases until it reaches \sim 120
 200 ns, where the time resolution is \sim 7.9 ps RMS, and apparently improves as
 201 the time difference increases further. This behavior is considered to be the
 202 constraint effect of the on-chip PLL and the domino-ring structure of the
 203 DRS4.

204 The linearity of the measured time is shown in Figure 10. Figure 10(a)
 205 shows the measured time difference with respect to the known value. The
 206 linearity in percentile is calculated by:

$$\text{Linearity}(\%) = \frac{\text{Measured time difference}}{\text{Known time difference at generator}} \times 100\% \quad (4)$$

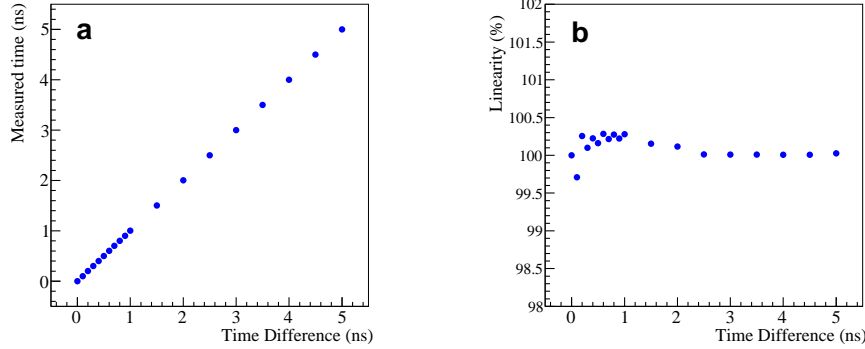


Figure 10: The linearity of the DRS4 time measurement. (a) The measured time difference in DRS4 vs. the time difference at AWG7102 generator. (b) The linearity in percentage as a function of the time difference.

207 Figure 10(b) shows the calculated linearity (%) as a function of the time
 208 difference, and the non-linearity is found to be smaller than 0.3% in the
 209 range of 0-2 ns time difference, and is smaller than 0.1% above 2 ns to 170
 210 ns (the figure only shows up to 5 ns). The results shown so far are obtained
 211 when operating the DRS4 board at 5 GS/s.

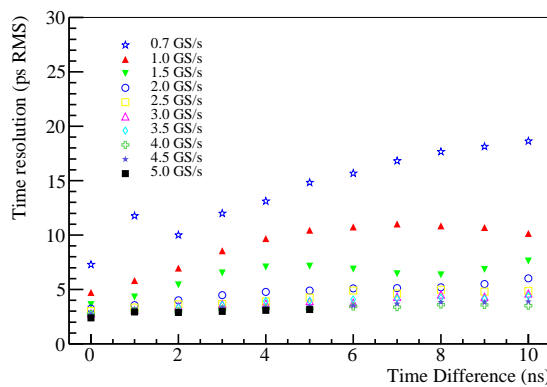


Figure 11: Electronic time resolution as a function of DRS4 sampling speed.

212 The Sawtooth calibration procedure is also repeated at other DRS4 sam-
213 pling speeds ranging from 0.7 to 5 GS/s, and the results on the time resolu-
214 tion are shown in Figure 11. The same sawtooth-shape pulse, described in
215 Section 2, is used for the time calibration at the different sampling speeds.
216 However, the width of the Gaussian pulses for measuring the time resolu-
217 tion is scaled in accordance with the sampling speed such that the number
218 of samples obtained for each pulse remains the same: e.g., the width of the
219 Gaussian pulses used for experiments conducted at 1 GS/s is 5 times the
220 width used for the experiments conducted at 5 GS/s (with a σ equal to 1
221 ns). The results in Figure 11 show that the time resolution dependencies at
222 all sampling speeds investigated are similar to that at 5 GS/s, especially in
223 the range of 2-5 GS/s. They also indicate that, as expected, the electronic
224 time resolution is smaller when a higher sampling speed is used, but the
225 differences from 2-5 GS/s are marginal.

226 *4.3. Results using PDRS4 board*

227 The Sawtooth time calibration method is applied for calibrating the
228 PDRS4 board [4] to check if the method is applicable to other waveform
229 electronics using the DRS4 chip. The PDRS4, shown in Figure 12(a), is a
230 prototype waveform readout board with 8 input channels developed for PET
231 application using the DRS4 chip. Following the same procedure and tests
232 described earlier for the DRS4 evaluation board, the electronic time resolu-
233 tion of the PDRS4 is measured and the result obtained at 5 GS/s is shown
234 in Figure 12(b). Compared to the result using a different calibration method
235 we previously reported [4], shown in Figure 1, the resolution dependence on
236 the time difference is reduced significantly, and the absolute resolution also is

improved. In comparison with the time resolution obtained with the DRS4 evaluation aboard using the Sawtooth time-calibration method, the result obtained with the PDRS4 has a worse time resolution and also shows a peak at about 2.5 ns time difference corresponding to its worst resolution within the 0-5 ns time difference range that we have investigated. We attribute the worse time resolution to a signal-to-noise ratio (SNR) difference: the noise level of the PDRS (~ 1.5 mV RMS) is larger than the DRS4 evaluation board (~ 0.4 mV RMS) [2][4], and the 1 V input dynamic range is fully used in PDRS4 while only half of it is used in the DRS4 evaluation board. This is consistent with the simplified rule for estimating the time resolution for waveform sampling given in [15]:

$$\sigma_t = \frac{t_r}{SNR\sqrt{N_{samples}}} \quad (5)$$

where t_r is the rise-time of the pulse and $N_{samples}$ is the number of samples within t_r . The cause of the particular shape of the PDRS4 curve is on the

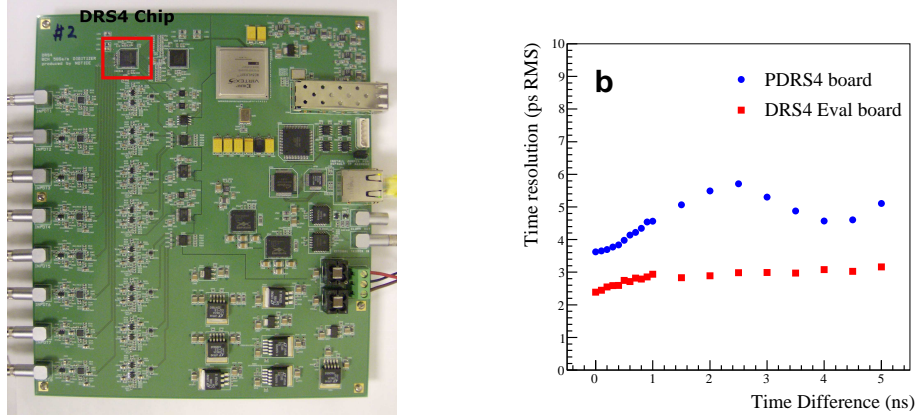


Figure 12: (a) PDRS4 board (b) Electronic time resolution of the PDRS4 measured by applying the new time calibration.

250 other hand unclear.

251 **5. Discussion**

252 The voltage linearity of the capacitor cells is an important factor in the
253 proposed time calibration method since the time interval between adjacent
254 capacitor cells is extracted from the differential voltage measurement un-
255 der the assumption of linear response in voltage. In this study, the voltage
256 calibration was carried out by the PSI software bundled with the DRS4 eval-
257 uation board. The voltage calibration uses two DC voltages (0 and 0.4 V)
258 for offset and gain correction for all 1024 capacitor cells, and the voltage
259 output is calculated by assuming linear response in the entire input dynamic
260 range of 1 V. Figure 13(a) shows the voltage linearity of the DRS4 evaluation
261 board to DC input voltages using the PSI voltage calibration. Each point in
262 the figure represents the collective response of the 1024 cells to the applied
263 DC offset voltages. 1000 events were acquired for each DC offset voltage

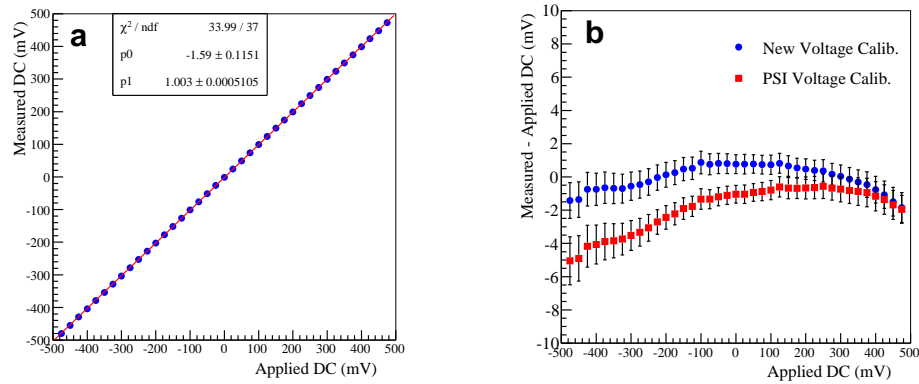


Figure 13: (a) Voltage linearity of the DRS4 evaluation board. (b) Voltage non-linearity after subtracting the applied DC value.

264 from -475 to 475 mV with a 25 mV step. The voltage non-linearity shown
265 in Figure 13(b) is calculated from the measured voltage output subtracted
266 by the known applied DC voltage. We have tested another voltage calibra-
267 tion method to demonstrate that the non-linearity can be reduced. In the
268 method, 39 different DC offset voltages in a range from -475 to 475 mV are
269 used, and the offset and gain for each cell is determined from the linear fit
270 on the measured responses. The voltage non-linearity measured by applying
271 the new voltage calibration is also shown in Figure 13(b). The variation
272 of non-linearity is reduced from $\sim 4\%$ to $\sim 2\%$ by applying the new voltage
273 calibration. Time resolution results in this study are using the PSI voltage
274 calibration and are expected to be improved with better voltage calibration.

275 A Tektronix AWG7102 waveform generator is used to generate the sawtooth-
276 shape pulse for time calibration in this study. The reasons for using the
277 AWG7102 are to produce a highly linear rising/falling pulse and measure the
278 electronic time resolution precisely, avoiding any possible effects from inac-
279 curate generators. To demonstrate that the method works well with other
280 lower-end pulse generators, we have also repeated the calibration by using
281 a Rigol DG4162 (160 MHz frequency) waveform generator [16]. In the test,
282 the rise time of the sawtooth-shape pulse was varied from 10 ns to 80 ns to
283 see any possible effects on the time resolution, and the sampling speed of the
284 DRS4 was fixed at 5 GS/s. The Gaussian pulse data set generated by the
285 AWG7102 is used here also for comparing the results. Table 1 summarizes
286 the time resolution obtained by using the time calibration constants obtained
287 from the sawtooth-shape pulses having rise time ranging from 10 - 80 ns for
288 three time differences: 1 ns, 5 ns, and 10 ns. The results show that the time

Pulse rise time	σ ($\Delta t = 1$ ns)	σ ($\Delta t = 5$ ns)	σ ($\Delta t = 10$ ns)
10 ns	2.8 ps	6.6 ps	7.9 ps
20 ns	3.0 ps	3.7 ps	4.5 ps
40 ns	2.9 ps	3.3 ps	4.3 ps
60 ns	2.9 ps	3.4 ps	4.6 ps
80 ns	2.9 ps	3.4 ps	4.0 ps

Table 1: Time resolutions (σ) obtained by using the time calibration constants obtained from the sawtooth-shape pulses with various rise time generated by the DG4162 for three time differences (Δt .)

289 resolution is not much affected by the rise time of the calibration pulse in the
 290 20 - 80 ns range. The worse time resolution obtained with 10 ns rise-time is
 291 considered to be an instrumental effect of the DG4162 generator.

292 In this study, 10K events of the sawtooth-shape pulse are used for the
 293 time calibration. Because of the plateau part of the pulse, the effective num-
 294 ber of calibration events is reduced by half to 5K, and the time calibration
 295 was carried out by using the ΔV histogram with ~ 5 K entries for each capac-
 296 itor cell. We have also checked how quickly the proposed Sawtooth method
 297 converges with the number of events used in calibration: the time calibration
 298 constants are calculated from the subset of the original 10K events, 250, 500,
 299 750, 1K, 2.5K, 5K and 7.5K, and the newly obtained calibrations are applied
 300 to measure the time resolution at time differences of 1, 5 and 10 ns, following
 301 the procedure described in Section 4.2. The DRS4 sampling speed is set to
 302 5 GS/s. Figure 14 shows the measured time resolution as a function of the
 303 number of calibration events. The results indicate that the time resolution

starts degrading when the number of calibration events is below 1K.

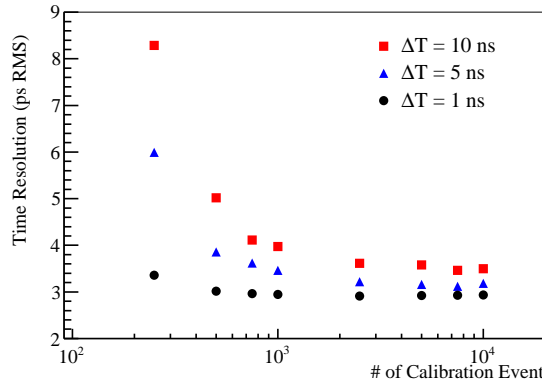


Figure 14: Time resolution as a function of the number of calibration events. Each point represents the time resolution measured by applying the time calibration constants obtained by using a subset of the original 10K events.

304
 305 According to the DRS4 chip specification [17], offset and gain errors due to
 306 temperature drift are reported to be $75 \mu\text{V}/^\circ\text{C}$ and $25 \text{ ppm}/^\circ\text{C}$ in 25 to 50°C ,
 307 respectively. We tested the stability of the time resolution of the DRS4 at
 308 three different temperatures: 28 , 33 and 44°C . The temperature drift during
 309 data acquisition, monitored by the on-board temperature sensor (MAX6662,
 310 MaximIntegrated) on the DRS4 evaluation board, was kept within 1°C . The
 311 time calibration constants obtained at these temperatures were applied to the
 312 same Gaussian pulse samples for time resolution measurement. The results,
 313 summarized in Table 2, show that the time resolution is stable to temperature
 314 changes in the range of 28 to 44°C . It is noted that in this experiment the
 315 sawtooth-shape pulses having a 10 ns rise-time for calibration were generated
 316 by using a Tektronix AFG3102 (100 MHz); the measured time resolutions are

317 again similar to the results obtained by using the time calibration constants
obtained with the AWG7102.

Temperature (°C)	σ ($\Delta t = 1$ ns)	σ ($\Delta t = 5$ ns)	σ ($\Delta t = 10$ ns)
28	2.9 ps	3.4 ps	3.9 ps
33	3.0 ps	3.5 ps	3.9 ps
44	2.9 ps	3.4 ps	3.8 ps

Table 2: Time resolutions (σ) measured for various time differences (Δt) by using the time calibration constants obtained when the DRS4 evaluation board is operated at three different temperatures.

318

319 **6. Summary**

320 We report a new time calibration method for DRS4-based waveform sam-
321 pling electronics. Based on the linearity of the sawtooth-shape pulse, the
322 method can calibrate the individual sampling intervals associated with the
323 1024 capacitor cells of the DRS4 from differential-voltage measurements. Af-
324 ter applying this method, the large variation in the sampling interval of the
325 DRS4 chip is clearly revealed. The dependence of the time resolution on the
326 time difference of two pulses, which has been observed by using other time
327 calibration methods, is significantly reduced after applying the proposed cal-
328 ibration method, and we are able to achieve 2.4 - 3.2 ps RMS time resolution
329 for the time difference in the 0-5 ns range. The proposed time calibration
330 method was applied to two different readout boards using the DRS4 chip
331 and could be applicable to other waveform sampling electronics based on
332 switched-capacitor-array technology.

333 **Acknowledgment**

334 This work was supported in part by the NIH grant R01EB016104, T32EB002103,
335 the University of Chicago and Fermilab strategic collaboration seed grants,
336 and the University of Chicago Institute for Translational Medicine awards.

337 **References**

338 [1] S. Ritt, R. Dinapoli, U. Hartmann, Nucl. Instr. and Meth. **623** (2010)
339 486.

340 [2] H. Kim, C.-T. Chen, H. Frisch, F. Tang, C.-M. Kao, Nucl. Instr. and
341 Meth. **662** (2012) 26.

342 [3] H. Kim et. al, IEEE NSS/MIC Conference Record (2012) 2466.

343 [4] H. Kim, C.-M. Kao, S. Kim, C.-T. Chen, IEEE NSS/MIC Conference
344 Record (2011) 2393.

345 [5] DRS4 Chip Home Page.

346 <http://www.psi.ch/drs/>

347 [6] DRS4 evaluation board software (verstion 4.0.1).

348 <http://www.psi.ch/drs/software-download>

349 [7] E. Delagnes, Y. Degerli, P. Goret, P. Nayman, F. Toussenel, P. Vincent,
350 Nucl. Instr. and Meth. **567** (2006) 21.

351 [8] G. Varner, L. Ruckman, A. Wong, Nucl. Instr. and Meth. **591** (2008)

352 534.

353 [9] E. Oberla, J.-F. Genat, H. Grabas, H. Frisch, K. Nishimura, G. Varner,
354 Nucl. Instr. and Meth. **735** (2014) 452.

355 [10] D. Breton, E. Delagnes, J. Maalmi, Proceedings of the Topical Workshop
356 on Electronics for Particle Physics (TWEPP-09) Prais:France (2009) -
357 <http://hal.in2p3.fr/in2p3-00421366>

358 [11] D. Breton, E. Delagnes, J. Maalmi, K. Nishimura, L. L. Ruckman,
359 G. Varner, J. Va'vra, Nucl. Instr. and Meth. **629** (2011) 123.

360 [12] K. Nishimura, A. Romero-Wolf, Physics Procedia **37** (2012) 1707.

361 [13] AWG7102 data sheet.
362 http://www.tek.com/sites/tek.com/files/media/media/.../76W_19779_3.pdf

363 [14] D. S. Shaver, presentation at IEEE NSS/MIC 2012 and private commu-
364 nication

365 [15] S. Ritt, DRS chip developments, Workshop on electron-
366 ics and DAQ for timing electronics in medical and par-
367 ticle physics, Clemont-Ferrand, France, January 2010,
368 http://www.psi.ch/drs/DocumentationEN/clermont_jan10.ppt

369 [16] Rigol DG4162 Waveform generator, [http://www.rigolna.com/products/waveform-](http://www.rigolna.com/products/waveform-generators/dg4162/)
370 [generators/dg4162/](http://www.rigolna.com/products/waveform-generators/dg4162/)

371 [17] DRS4 chip specification sheet.
372 http://www.psi.ch/drs/DocumentationEN/DRS4_rev09.pdf